Optimizing the electrolyte and binder composition for Sodium Prussian Blue, $Na_{1-x}Fe_{x+(1/3)}(CN)_6 \cdot yH_2O$, as cathode in sodium ion batteries

Mª José Piernas-Muñoz [a], E. Castillo-Martínez [a,*] J. L. Gómez-Cámer [a,1], T. Rojo [a, b,*]

[a] CICenergigune, Parque Tecnológico de Álava, Albert Einstein 48, ED. CIC, 01050 Miñano, SPAIN. ecastillo@cicenergigune.com

[1] ISE member

[b] Departamento de Química Inorgánica, Universidad del País Vasco UPV/EHU, P.O. Box 664, 48080 Bilbao, SPAIN. trojo@cicenergigune.com

Abstract

Na-ion batteries (SIB) are now attracting researcher´s attention as possible substitutes of the Li-ion batteries. Promising cathode materials, which have demonstrated to work well for SIB are those based on the sodiated Prussian Blue, $NaFeFe(CN)_6$, Prussian White, $Na_2FeFe(CN)_6$, and their analogues. Herein, the effect of different electrolytes and binder composition, on the electrochemical performance of sodium Prussian Blue, $Na_{0.75}Fe_{2.08}(CN)_6 \cdot 3.4H_2O$, as cathode material for SIB is studied. Several electrolytes containing $NaClO_4$ or $NaPF_6$ salts in carbonated mixtures, with and without fluoroethylene carbonate (FEC) as additive, have been tested for $Na_{0.75}Fe_{2.08}(CN)_6 \cdot 3.4H_2O$. The effect of different binders, polyvinylidene fluoride (PvdF), sodium carboxymethyl cellulose (CMC), polytetrafluoroethylene (PTFE) and ethylene propylene diene monomer ruber (EPDM), is also investigated.

Highlights

- Sodium Prussian Blue (Na-PB) is used as cathode in sodium ion batteries (SIB).
- Several electrolytes and binders are electrochemically tested for Na-PB.

- 1M $NaPF_6$ in EC: PC: FEC can be established as standard electrolyte for Na-PB.
- PVDF is the advisable binder for Prussian Blue cathode materials in SIB.

Keywords: Electrochemical energy storage, Prussian blue, cathodes, Na-ion batteries, electrolyte effect, binder effect.

1.) Introduction

Concerns about the huge amount of energy we consume nowadays, leads to the urgent necessity of finding a new technology that can efficiently and repeatedly store and release this energy at low cost and safely. In this context, rechargeable, low-cost batteries have demonstrated during the last decades to be an adequate tool for this purpose. Because of their high performance, lithium ion batteries (LIB), such as those based on $LiCoO_2$, $LiMn_2O_4$ and $LiFePO_4$, among others, are so far the most common battery chemistries employed for new technological applications, such as portable electronic devices or electric vehicle industry. They are also becoming a reality for some large-scale applications, as for example in Kauai island electric grid, enabling the integration of non-continuous but clean renewable sources. [1, 2]

For large scale applications, new tendencies are however moving toward developing electrode materials on the basis of abundance, availability and, subsequently, lower price.[2] In this sense, sodium ion batteries (SIB) are emerging as a strong alternative for LIB, mainly for large scale applications, since these deploy more environmentally friendly materials (sodium is the 4^{th} most abundant element on the Earth) and maintenance costs would be lower. Despite the apparent similarities between Li and Na chemistries, important differences have been found in the electrochemical performance

of both. As a consequence of the bigger size of Na^+, it is necessary the use of host structures with a larger interstitial space than for Li^+ to allow ion diffusion.[3] In addition, the more positive reduction potential of Na^+ with regard to Li^+ (-2.71 V and -3.05 V *vs.* S.H.E., respectively), entails lower energy densities, nevertheless this is not the most critical parameter for large storage applications. [4, 5, 6, 7]

A wide number of compounds: layered transition metal oxides,[8, 9, 10, 11] Na super ionic conductor (NASICON and derivates), fluorophosphates[12, 13, 14] and fluorosulphates,[15] have been studied as positive electrodes for room temperature SIB.[16] Nonetheless, an alternative material that aligns with the low cost philosophy of SIB is Prussian Blue (PB), which is synthesized in aqueous media and usually at room temperature.

PB, ideally, $AM(Fe(CN)]_6 \cdot mH_2O$ (A=alkali ion (Li^+, Na^+, K^+), M=transition metal), presents a host structure with tunable, open channels that allow rapid insertion of species.[17] It has a cubic framework (space group $Fm\bar{3}m$) with Fe(II) and Fe(III) on alternate corners of a cube of corner-shared octahedral bridged by linear $(C\equiv N)^-$ anions. The linear $(C\equiv N)^-$ molecule gives an M(II)–N≡C–Fe(III) bond length of about 5Å that allows Na^+ ions to be inserted reversibly into the empty large-ion sites.[18, 19] In addition to its easiness of synthesis and safety, it can deliver the theoretical specific capacity of 170 mAh g^{-1} when achieving the complete reduced form, $Na_2Fe_2(CN)_6 \cdot nH_2O$ (Prussian White, PW), since it involves the insertion/de-insertion of $2Na^+$ per formula unit with the consequent $2e^-$ redox process.[20, 21, 22]

Prussian Blue and its analogues, $AMFe(CN)_6 \cdot xH_2O$ (A= K/Na, M= Mn/ Fe/ Co/ Ni/ Zn), have been studied as cathode materials for SIB. Reversible capacities of ~ 56 mAh g^{-1} were achieved when A= Na and M= Zn.[23] However, if A= K and M= Fe, ~100

mAh g^{-1} were exhibited during discharge.[19, 24] Specific capacities of up to 170 mAh g^{-1}, with no apparent capacity loss for 150 cycles have been obtained when high-quality PB nanocrystals, $Na_{0.61}Fe[Fe(CN)_6]_{0.94}\square_{0.06}$, with almost no zeolitic water and no $[Fe(CN)_6]$ vacancies content, are used. [25]

Moreover, PB related phases have been tested as positive electrodes for insertion/de-insertion of Na^+. Single-crystal nanoparticles of Berlin Green (BG), $FeFe(CN)_6,\cdot H_2O$, displayed 120 mAh g^{-1} (corresponding to 1.52 Na^+ insertion) and a maintained coulombic efficiency of ~ 100% for more than 600 cycles.[26]

Apart from differences inherent to the materials, such as those due to the chemical composition or crystal size which depends on synthesis conditions, the studies previously described for PB, BG, PW and its analogues have been carried out using different electrolytes, as $NaClO_4$ or $NaPF_6$ dissolved in different mixtures of carbonated compounds, as PC, EC: DMC (1:1), EC: DEC (1:1), remaining unclear the influence of the electrolyte on their electrochemical performance. However, it is well known that the proper performance of the battery is not only dependent on the electrode materials but also strongly subject to the electrolyte election. The ion mobility, related to the viscosity and ionic conductivity, as well as the thermal and electrochemical stability of the electrolyte, are primary parameters for finding a suitable electrolyte and change from one mixture/composition to other.[27, 28, 29, 30] Consequently, to find a standard electrolyte providing optimum features that could contribute to homogenize the results and, therefore, facilitate the comparison among the electrochemical properties of the different Prussian Blue compounds is desirable. Furthermore, the choice of the binder also plays an important role in the cycling stability and rate capability of the battery.[31] Several studies with other binders different from the universal used in LIB applications,

polyvinylidene fluoride (PVDF), such as carboxymethyl cellulose (CMC),[32] polyacrylic acid (PAA),[33] alginate[34] and ethylene propylene diene monomer (EPDM),[35] among others, have proved to enhance the cycling performance of the cell.

The scope of this work is to determine the optimum electrolyte and binder for Na-PB when used as cathodic electrode in SIB, to be stablished as standards for future studies with PB related (PB Analogues, PW, BG) or, even, possible market applications. For this purpose, herein we report on the synthesis and electrochemical studies of microsized low cost Sodium Prussian Blue, $Na_{0.75}Fe_{2.08}(CN)_6 \cdot yH_2O$, as cathode material in sodium ion batteries with different electrolyte and binder compositions.

2.) Experimental Section

2.1. Synthesis

2.1.1. Sodium Prussian Blue synthesis

The Sodium Prussian Blue phase was obtained following the same method that we previously reported for Potassium Prussian Blue, except that the sodiated starting cyanide was used instead of the potassium analogue.[36] In a typical experiment, aqueous $Na_4Fe(CN)_6 \cdot 10H_2O$ solution (0.04 M) and $FeCl_3 \cdot 6H_2O$ solution (0.04 M) were prepared separately. Commonly, 100 mL of the $Na_4Fe(CN)_6 \cdot 10H_2O$ solution were mixed with 100 mL of $FeCl_3 \cdot 6H_2O$ instantaneously generating a dark blue coloured suspension containing $Na_{1-x}Fe^{III}_{1+(x/3)}[Fe^{II}(CN)_6] \cdot yH_2O$, as the following reaction depicts:

$$(1 + (x/3))\ FeCl_3 + Na_4[Fe(CN)_6] \cdot 10H_2O \rightarrow Na_{1-x}Fe^{III}_{1+(x/3)}[Fe^{II}(CN)_6] \cdot yH_2O + (3 + x)\ NaCl \qquad \text{(Eq. 1)}$$

As a consequence of the small particle size, due to the brief nucleation time, addition of ethanol to the suspension was necessary in order to facilitate/force the precipitation of the $Na_{1-x}Fe^{III}_{1+(x/3)}[Fe^{II}(CN)_6]\cdot yH_2O$, hereinafter abbreviated as Na-PB. After filtering for 48 h, washing again with ethanol (3x10 mL) and drying the precipitate, dark blue Na-PB crystal-like microparticles were obtained.

2.2. Structural characterization

PXRD data were collected in a Bruker D8 Advance X-Ray diffractometer, with λ (CuKα)=1.54056 Å. The measured data range extends from 5° to 80°, 2θ, with a step size width of 0.0194°. IR spectra were recorded in the range of $\bar{\nu}$ = 4000 – 650 cm^{-1} in absorption mode using an Agilent Cary 630 FTIR spectrometer (Agilent Technologies), situated inside an Ar-filled glove box, provided with a Ge ATR, by directly placing the powdered material in a 5 bounce ZnSe sampling window. Scanning Electron Microscopy (SEM) was utilized to study the morphology and particle size of Na-PB. SEM was performed in a FEI Quanta 200F SEM operated at 30kV and equipped with an Apollo 10 SSD Energy Dispersive X-ray (EDX). Elemental analysis (H, C, N) was carried out in a Euro Elemental Analyser (CHNS), to check the H, C and N percentage present in the compound. TGA NETZSCH STA 449 F3 Jupiter was used to collect the thermogravimetric curve of Na-PB. TGA experiments were performed in the temperature range from 30 to 325°C using N_2 atmosphere and a temperature step of 10 K min^{-1} (see Figure S1). The molar Na: Fe ratio of the sodium iron hexacyanoferrate was obtained by atomic absorption (AA) spectroscopy.

2.3. Electrochemical characterization

2.3.1. Electrochemical characterization of Na-PB

For testing the electrochemical performance of Na-PB versus sodium, galvanostatic measurements were conducted at room temperature in the voltage window from 2.4 to 4.2 V in a battery and cell test equipment (MACCOR Series 4000 Battery Tester). Two-electrode coin-type half cells (CR 2032 type) were assembled. For the electrolyte election, positive electrodes consisted of 80 wt% Na-PB, 10 wt% Super C65 and 10 wt% poly(vinylidene fluoride), mixed with N-methyl-2-pyrrolidone (NMP). Electrochemical impedance spectroscopy analyses were carried out in three-electrode Swagelok type cells with the aforementioned positive electrode and a Na metal disc as counter electrode. A small metallic Na piece was used as reference electrode placed between two Whatman GF-D glass fibre separators soaked in the corresponding electrolyte. The impedance measurements were recorded in the frequency range from 100 KHz to 10 mHz with an amplitude of 10 mV in a Biologic VMP3 potentiostat.

When the binder effect was studied, positive electrodes were prepared by mixing Na-PB with amorphous carbon (Super C65) and the binder dissolved in their corresponding solvent in an 80:10:10 ratio. Typically, the slurries were then casted on Al foil and dried under vacuum at 80°C overnight. Disc electrodes were punched, pressed at 5 tons and dried under vacuum again at 80°C overnight. Metallic sodium was used as a negative and counter electrode. Electrodes were galvanostatically cycled at C/10, 1C, 10C and C/10 fixed current densities, based on a theoretical capacity of 1C = $C_{Na\text{-}PB,th}$=92.19 mAh g^{-1} corresponding to the insertion of 1 Na^{+}/f.u. Typical cell loadings were 1.5-3 mg of active material per coin cell. Reported data are single run for typical results.

2.3.2. Electrolyte election

To determine the most appropriate electrolyte for Na-PB, several mixtures (see Table 1), such as 1M $NaClO_4$ in ethylene carbonate: propylene carbonate (EC: PC) 50:50, 1M $NaClO_4$ in ethylene carbonate: dimethyl carbonate (EC: DMC) 50:50, 1M $NaClO_4$ in ethylene carbonate: diethyl carbonate (EC: DEC), 1M $NaPF_6$ in EC: PC 50:50, 1M $NaPF_6$ in EC: DMC 50:50, 1M $NaPF_6$ in EC: DEC 50:50, with and without a 2% of fluorinated ethylene carbonate (FEC) as electrolyte additive, were deployed impregnating the glass fibre filter paper (Whatman, GF-D) used as separator.

The electrolytes selection criteria were based on the compilation of those usually used in the laboratory, and those already reported in the literature.

2.3.3. Binder election

Once the electrolyte providing the best electrochemical properties of microsized Na-PB was deduced, the binder selection was carried out. The binders tested were Solef® PVDF dissolved in NMP, sodium CMC M.W. ca. 250000 g/mol, Sigma Aldrich, dissolved in ethanol / H_2O, 60 wt. % polytetrafluoroethylene (PTFE) dispersion in H_2O, Sigma Aldrich, dispersed in ethanol and EPDM rubber 50 wt. % dissolved in cyclohexane. A glass fibre filter paper (Whatman, GF-D), impregnated with $NaPF_6$ 1M in ethylene carbonate: propylene carbonate containing FEC (EC: PC: FEC 49:49:2), was used as separator.

3.) Results and discussion

3.1. Structural characterization

The powder X-ray diffractogram (PXRD) confirms the formation of Na-PB. The broadening of the reflections could indicate the possible formation of nanoparticles, as a

consequence of the fast nucleation when the reaction takes place. Fig.1a illustrates the profile matching plot of Na-PB (space group (*Fm*-3*m*)). The fitting has been performed without refining the atomic positions and results in a lattice parameter a= 10.2227 (1) Å. Agreement factors were, R_B= 2.92, R_F= 3.88 and χ^2=16.4.

Infrared spectrum (see Fig.1b) indicates the presence of the cyanide (-C≡N) stretching vibrational band for Na-PB at 2076 cm^{-1}. SEM images show the homogeneous micron-sized particle size distribution (Fig. 1c and d). The particle size observed in SEM is larger than the ≈ 13.5 nm calculated by Debye-Scherrer from the width of the PXRD reflections. This suggests aggregation of nanocrystalline domains into larger microparticles. Semiquantitative EDX analysis reveals an estimated 1:2 Na: Fe ratio for Na-PB. However, a more accurate composition of the material was determined by atomic absorption spectroscopy (AAS) and elemental analysis (H, C, N). Water content present on the material was obtained by TGA (see Fig.S1). The molecular formula achieved was $Na_{0.75}Fe_{2.08}(CN)_6 \cdot 3.4H_2O$.

3.2. Electrochemical performance of Na-PB

3.2.1. Electrolyte election

The electrochemical performance of Na-PB was optimized in terms of electrolyte and binder composition, which could be extended, in principle, to other PBA materials acting as cathode in Na-ion batteries. To determine which electrolyte provides the best results for this material at the selected voltage range from 2.4 to 4.2 V, several carbonate based electrolyte mixture solutions, including those electrolytes previously used for PBA, were tested: 1 M $NaClO_4$ in EC: PC 50:50, 1 M $NaClO_4$ in EC:DMC 50:50, 1 M $NaClO_4$ in EC: DEC 50:50, 1 M $NaPF_6$ in EC:PC 50:50, 1M $NaPF_6$ in EC:DMC 50:50, 1M $NaPF_6$ in EC:DEC 50:50, with and without a 2% of FEC as electrolyte additive. Other sodium

salts, different from $NaClO_4$ or $NaPF_6$, such as NaTf (sodium triflate), NaFSI (sodium bis(fluorosulfonyl)imide) or NaTFSI (sodium bis(trifluoromethanesulfonyl)imide), were not considered in this study as a result of the corrosion problem they present with the aluminium current collector.[29]

Fig. 2a illustrates the first galvanostatic discharge and the second galvanostatic charge profiles of Na-PB versus Na at C/10, considering 1C = $C_{th,\ Na\text{-}PB}$ = 92.185 mAh/g corresponding to the insertion of 1 Na^+/f.u., when some of the different electrolytes previously listed, $NaClO_4$ or $NaPF_6$ in different carbonate mixtures, are deployed (see Fig. S2 for further information about the electrochemical performance when using the rest of electrolytes above mentioned and Table S1 for further information about the specific charge values obtained for each electrolyte). The initial phase contains 0.75 Na, and therefore, on the first oxidation of Na-PB to Berlin Green, $Fe_2(CN)_6$, only less than one sodium can be de-inserted. Consequently, the first charge is not shown. Two plateaus are easily distinguished both in charge at ca. 2.95 and around 3.65 V and in discharge at ~2.8 and ~3.4 V and a significant difference of 23.5% is observed between the electrolytes providing the higher and the lower specific charge at C/10 (see Figure S4 for further information). From now on, all the given specific charge values will be referred to the insertion of sodium.

Rate capability tests, consisting on ten cycles at each one of the following subsequent C-rates: C/10, 1C, 10C and again C/10, were conducted for Na-PB, and are displayed in Fig. 2b and c, with the electrolytes containing $NaClO_4$ or $NaPF_6$ plotted separately for clarity. The largest reversible specific charge, in each and every one of the C-rates (C/10, 1C and 10C), was achieved with EC: PC 50:50 and EC: DMC: FEC 49:49:2 for the $NaClO_4$ containing electrolyte. Both solvent mixtures approximately

exhibited 125 mAh g^{-1} at C/10, 100 mAh g^{-1} during the following 10 cycles run at 1C and about 55 mAh g^{-1} when cycled at 10C (922 mA g^{-1}). On the order of 120 mAh g^{-1} were recovered by 1M $NaClO_4$ EC: DMC: FEC 49:49:2 when coming back to C/10. Although by using $NaClO_4$ in the mixture EC: DEC: FEC 49:49:2 similar specific charge are achieved along the first 10 cycles, when the current densities are increased, the specific charge (89.5 and 41.4 mAh/g at 1C and 10C, respectively) was not as good as that obtained with EC: PC 50:50. With respect to the electrolytes that contained $NaPF_6$, EC: PC 50:50 and EC: PC: FEC 49:49:2 enabled Na-PB to reach specific charge values up to 140 and 130 mAh g^{-1}, respectively, when cycled at C/10. Even 110 mAh g^{-1} at 1C and 65 mAh g^{-1} at 10C were achieved in the case of the 1M $NaPF_6$ EC: PC 50:50, but this mixture showed the largest fading. It is important to remark that the mass loading parameter is not affecting the measurements performed at high C-rates, as shown in figure S5.

Focusing on the four electrolytes that showed the higher discharge specific capacities at the different C-rates (marked in bold in Table 1 and with the symbol † on its right): 1M $NaClO_4$ in EC: PC 50:50, 1M $NaClO_4$ in EC: DMC: FEC 49:49:2, 1M $NaPF_6$ in EC: PC 50:50 and 1M $NaPF_6$ in EC: PC: FEC 49:49:2, other important parameters such as the coulombic efficiency (Qeff) (Fig. 3a-e) and the capacity retention (Fig. 3f) were studied in detail. Figure 3b shows a Qeff ≥97% for all the electrolytes when cycled at C/10 except for $NaClO_4$ 1M in EC: PC 50:50. For this latter, the efficiency is lower than 95% which is not appropriate for battery operation. The other electrolyte without FEC additive, $NaPF_6$ 1M in EC: PC 50:50 also displayed lower Qeff (98%) at high rates of 1C when compared with the other two electrolytes (99.5%), and even decreased down to 97% at the highest C-rate, 10C, which is far from the satisfactory 99.85% displayed by $NaClO_4$ 1M EC: DMC: FEC 49:49:2 and $NaPF_6$ 1M EC: PC: FEC 49:49:2. In general, it can be observed a better Qeff, apart from an improved capacity, for those electrolytes

containing FEC as electrolyte additive (Fig. 3), that leads to an enhanced stabilization between the charge and discharge processes during cycling. As summary, the two electrolytes that showed the highest capacity and Qeff for Na-PB are 1M $NaClO_4$ in EC: DMC: FEC 49:49:2 and 1M $NaPF_6$ in EC: PC: FEC 49:49:2.

Regarding the capacity retention (Figure 3f), although both FEC containing electrolytes show similar retention of the initial capacity at low C-rates, it is noticeable that $NaPF_6$ 1M in EC: PC: FEC 49:49:2 displays a more stable behavior at high C-rates and during the last 10 cycles at C/10. In addition, $NaClO_4$ presents explosive hazards for a real application and should be preferably avoided. Consequently, we can state that the most suitable organic liquid electrolyte for testing Na-PB electrochemically vs Na, in the voltage from 2.4 to 4.2 V, is 1M $NaPF_6$ EC: PC: FEC 49:49:2.

Figure 4a-d shows the electrochemical impedance spectra recorded for the 4 shortlisted electrolytes (highlighted in bold in Table 1 and containing the symbol †) at the end of discharge (EOD), i.e. at 2.4 V vs Na^+/Na, after each of the first five cycles. Na-PB electrodes cycled in $NaClO_4$ based electrolytes (Figure 4a and b) exhibit impedance profiles which evolve upon cycling whereas those cycled in $NaPF_6$ based electrolytes (Figure 4c and d) the total impedance is more stable regardless of the presence of FEC additive. At first sight, a clear difference between both salts can be observed from the impedance response.

The EIS spectra of Na-PB cycled in 1M $NaClO_4$ in EC: PC and 1M $NaPF_6$ in EC: PC: FEC (4b and d) were fitted with an equivalent circuit with three RC elements (see Figure 4e inset). The other two samples (1M $NaClO_4$ in EC: DMC: FEC and 1M $NaPF_6$ in EC: PC, Figure 4a and c, respectively) admitted fitting with only two RC elements. These two possibilities exhibited different error level, having the proposed equivalent

circuit larger relative error but smaller statistical parameter χ^2 than the circuit with only two RC elements. Since the electrodes were all from the same coating/laminate and were carefully chosen to have similar mass and thickness leaving the electrolyte as the only varying parameter, we decided to maintain the same equivalent circuit for all samples. In all the analyzed spectra the χ^2 parameter was kept below $9 \cdot 10^{-4}$. Two semicircles appear at high frequency, which could be assigned to the presence of surface films, however the capacitances calculated are several orders of magnitude lower than expected ($\sim$ 5-10 μF cm^{-2}). Another possible explanation for the high frequency semicircle is the contact resistance between the electrode material and the Al current collector.[37] In our case, the only difference between samples is the electrolyte solvents and salt, which could certainly affect the passivation of the Al current collector and the contact resistance but further investigations are needed to prove it.

Since the origin of high frequency response is unclear we compared all Na-PB samples by their total resistivity, $R_a+R_b+R_{ct}$ (R_a: resistance component a, R_b: Resistance component b, R_{ct}: charge transfer resistance).[38] Figure 4e shows the total resistivity of the Na-PB samples cycled in the four studied electrolyte combinations. Na-PB cycled in $NaClO_4$ based electrolytes showed low resistivity and different behaviour upon cycling. The 1M $NaClO_4$ in EC: DMC: FEC electrolyte results in higher resistivity than in EC: PC but with more stable response. This could explain the stronger fading of 1M $NaClO_4$ in EC: PC and its worse capacity retention after the high C-rate capability test (Figure 2b). On the other hand, $NaPF_6$ based electrolytes exhibited great stability after 5 cycles, especially the 1M $NaPF_6$ in EC: PC: FEC which showed much lower resistivity than without FEC additive. These results seem to contradict the better cycling performance of 1M $NaPF_6$ in EC:PC (Figure 2c), however at high C-rate their specific charge becomes

similar and Qeff gets worse but more stable cycling can be obtained with FEC at 10C and afterwards.

These results are in agreement with those previously described in the literature, that claim that PF_6^- anion is a more suitable salt for cathodic studies than the ClO_4^-, as a consequence of its higher resistance to oxidation.[30] Our electrolyte election is also consistent with Palacin´s report establishing that $NaPF_6$ in EC: PC possessed all the features to be adopted as standard electrolyte for Na-ion batteries,[27] with the highest thermal and electrochemical stability from a wide variety of carbonate mixtures. Moreover, the addition of a small percentage of an additive, FEC, enhances the capacity retention and the Qeff in anode materials for SIBs, as Komaba demonstrated for the first time for hard carbons.[3940] Although there are contradictory results related to hard carbons, other anode investigations revealed an enhanced electrochemical stability when FEC is added.[41] Furthermore, recent studies also proved an improvement in the cycling stability of cathodes in LIB when using FEC, as a result of the formation of SEI components on the cathode surface. This surface is abundant in polycarbonate components that enhance the ionic conductivity of the SEI film and reduces the electrode/electrolyte interfacial impedance.[42, 43] To the best of our knowledge, this is the first report on the influence of FEC on cathode performance for SIB. We observe a decrease in the interfacial resistivity when FEC is added. We are hereby showing its beneficial effect in cathode performance for sodium ion batteries.

3.2.2. Binder election

We proceed then to determine the binder that enables the optimum electrochemical performance of Na-PB, using the selected electrolyte, 1M $NaPF_6$ EC: PC: FEC 49:49:2, in the same voltage window, from 2.4 to 4.2 V *vs.* Na^+/Na. As explained, positive electrodes were prepared with a 10% of different binders in the appropriate solvent. PVDF in NMP, Na-CMC in EtOH / H_2O, PTFE in H_2O/EtOH and EPDM in cyclohexane were the binders tested. Disc electrodes coated over Al foil, were punched, pressed at 5 tons and dried under vacuum again at 80°C overnight, except for PTFE, which was self-standing.

When Na-PB slurry is prepared with Na-CMC as binder dissolving it in H_2O, the mechanical properties of the electrodes are not adequate, i.e., when the mixture is extended over the current collector foil, a total lack of wettability and adherence to the metal is observed, probably due to the partial solubility of Na-PB in H_2O, which forms a colloidal suspension with high surface tension. If the slurry is, however, prepared using EtOH as solvent and adding few drops of H_2O, the previous problem is solved. It seems that EtOH, which is the solvent used to force the precipitation of Na-PB, avoid the partial dissolution of Na-PB and electrodes completely stuck to the foil are achieved.

It is worth mentioning that the highest capacities, both at low and high current densities, were achieved by using PVDF as binder (see Figure 5) while EPDM displayed the worst behaviour (see S7 and S8). The PVDF based NaPB electrodes exhibit specific charges of up to 130 mAh g^{-1}, Qeff of nearly 99% after 30 cycles and 87% of capacity retention at the end of the rate capability test (after 40 cycles). Surprisingly, CMC also exhibits fairly good capacities at high C-rates (ca. 53 mAh g^{-1} at nearly 1 A g^{-1}). These results are consistent with those reported by Chou et al.[31] Although some water based binders have proved to work better for anodes in contrast to PVDF, the replacement of PVDF by envorinmentally friendly aqueous based binders in cathodes, such as CMC or

PTFE, presents some difficulties which are believed to be related to the lack of stability of the cathode in water, as well as the slurry formulation, the control on the viscosity and the way of processing the film.[31] It is worth noting that the electrolyte-binder combination is crucial for achieving the optimum performance and therefore if a different electrolyte is used another binder might outperform PVDF´s results.

In an attempt to explain the varied electrochemical behaviour observed depending on the binder deployed in each case, images of the cross-section of the electrodes were recorded by SEM. The study of the cross-section provides an idea of the adherence existent between the active material/conducting additive/binder mixture (electrodic layer hereafter) and the current collector, which is a determining parameter for an adequate electrical contact.

When PVDF is used as binder (Fig. 6a and b), no clear separation between both phases is observed. The electrodic layer seems perfectly glued to the Al foil, resulting in good electrical contact, as it is also evidenced by its electrochemical results (highest capacities at all C-rates). With CMC (Fig. 6c and d), the adherence is also good although at some points a small void space is distinguished between the electrode material and the current collector. PTFE (Fig. 6e and f) was prepared as self-standing electrode, without using current collector. The larger thickness of this electrode can explain its fading when it is cycled at high current densities as 1 A g^{-1}. However, in EPDM (Fig. 6g and h), we can easily differentiate 2 zones, a thinner layer (≈ 20 micron) of electrodic layer adhered to the current collector and a thicker layer (≈ 40 micron) clearly separated, revealing a lack of electrical contact, that could be the explanation for the low capacities it exhibits at moderate and high current densities.

To sum up, it is evident that comparing all the binders, PVDF and EPDM are, respectively, those with best and worse contact, what is in agreement with their corresponding electrochemical performance. Apart from the adherence, the influence of the functional groups, present on the binders, is also critical for the electrochemical behaviour and would constitute an interesting study to develop in a near future.

Conclusions

Several electrolytes containing $NaClO_4$ or $NaPF_6$ salts in carbonated mixtures (EC:PC, EC:DMC), with and without a small amount of FEC as additive, have been electrochemically tested for sodium Prussian blue, $Na_{0.75}Fe_{2.08}(CN)_6 \cdot 3.4H_2O$ when laminated with PVDF as binder. The most suitable organic electrolyte for testing Na-PB in SIB, in the voltage range from 2.4 to 4.2 V, is $NaPF_6$ 1M EC: PC: FEC 49:49:2, exhibiting one of the highest reversible specific charge (130 mAh g^{-1}), with 99.5% of Qeff and 87% of capacity retention after the C-rate capability test (40 cycles). This agrees with the lower interfacial resistance observed for this electrolyte mixture. The influence of different binders (PVDF, CMC, PTFE and EPDM), in the electrochemical performance of sodium PB has been studied as well. PVDF has clearly displayed the best results in terms of specific charge (130 mAh g^{-1}), Qeff (nearly 99% after 30 cycles) and capacity retention (87% after the C-rate capability test). We consider that the use of this electrolyte and binder can also be extended to other PB analogues and derived, providing optimum features and also contributing to homogenize the results and, therefore, facilitating the comparison of the electrochemical properties among the different PB compounds. Other option to contemplate is the possible use for market applications and the extension to other SIB systems.

Acknowledgments

This work was financially supported through projects ENE2013-44330-R and Etortek 14 CIC Energigune. SGIker technical and human support (UPV/EHU, MICINN, GV/EJ, ESF) is gratefully acknowledged because of the help with AAS and elemental analysis (H, C, N). The authors would also like to acknowledge Egoitz Martín and Jon Ajuria, for their help with XRD data and SEM images collection, respectively. Mª José Piernas Muñoz thanks the Basque Government for the grant corresponding to "Nuevas Becas y renovaciones para el Programa Predoctoral de Formación de Personal Investigador" (PRE.2013.1.790, MOD A) and the funding through Etortek project Energigune '14, LINABATT (ENE2013-44330R). Juan Luis Gómez Cámer thanks the Spanish Government (Ministerio de Economía y Competitividad) for the grant "Ayudas Juan de la Cierva – Incorporación IJCI-2014-20613".

Notes and references

[a] CICenergigune, Parque Tecnológico de Álava, Albert Einstein 48, ED. CIC, 01050 Miñano, SPAIN. ecastillo@cicenergigune.com

[b]Departamento de Química Inorgánica, Universidad del País Vasco UPV/EHU, P.O. Box 644, 48080 Bilbao, SPAIN. trojo@cicenergigune.com

Electronic Supplementary Information (ESI) available: [details of any supplementary information available should be included here]. See DOI: 10.1039/c000000x/

[1] Armand M., Tarascon J-M. Nature 451 (2008) 652-657.

[2] Dunn B., Kamath H., Tarascon J-M. Science 334 (2011) 928-935.

[3] Long Wang, Yuhao Lu, Jue Liu, Maowen Xu, Jinguang Cheng, Dawei Zhang, John B. Goodenough. Angew. Chem. Int. Ed. 52 (2013) 1964-1967.

[4] Kim S-W., Seo D-H., Ma X., Ceder G., Kang K. *Adv. Energy Mater*. 2 (2012) 710–721.

[5] Palomares V., Serras P., Villaluenga I., Hueso K., Carretero-Gonzalez J., Rojo T. En. Environm. Sci. 5 (2012) 5884-5901.

[6] Palomares V., Casas-Cabanas M., Castillo-Martínez E., Han M. H., Rojo T. Energy Environ. Sci. 6 (2013) 2312–2337.

[7] Yabuuchi N., Kubota K., Dahbi M., Komaba S. Chem. Rev. 114 (2014) 11636−11682.

[8] M. H. Han, E. Gonzalo, G. Singh, T. Rojo. Energy and Environ. Sci. 8 (2015) 81-102.

[9] G. Singh, J. M. López del Amo, M. Galcerán, S. Pérez-Villar, T. Rojo. J. Mater. Chem. A 3 (2015) 6954-6961.

[10] E. Gonzalo, M. H. Han, J.M. López del Amo, B. Acebedo, M. Casas-Cabanas, T. Rojo. J. Mater. Chem. A 2 (2014) 18523.

[11] K. Kubotaa, N. Yabuuchia, H. Yoshidaa, M. Dahbia, S. Komaba. MRS Bulletin 39 (2014) 416-422.

[12] N. Sharma, P. Serras, V. Palomares, H. E. A. Brand, J. Alonso, P. Kubiak, M. L. Fdez-Gubieda, T. Rojo. Chem. Mater. 26 (2014) 3391-3402.

[13] P. Serras, V. Palomares, T. Rojo, H. E. A. Brand, Neeraj Sharma. J. Mater. Chem. A 2 (2014) 7766 .

[14] P. Serras, V. Palomares, J. Alonso, N. Sharma, J. M. López del Amo, P. Kubiak, M. L. Fdez-Gubieda, T. Rojo. Chem. Mater. 25(2013) 4917−4925.

[15] C. Masquelier, L. Croguennec. Chem. Rev. 113 (2013) 6552–6591.

[16] J. Xu, D. H. Lee, Y. S. Meng. Funct. Mat. Lett. 6 (2013) 1330001.

[17] Colin D. Wessells, R. A. Huggins, Y. Cui. Nature Comm. 2 (2011) 550.

[18] J. F. Keggin, F. D. Miles. Nature (1936) 577.

[19] Y. Lu, L. Wang, J. Cheng, John B. Goodenough. Chem. Commun. 48 (2012) 6544-6546.

[20] You Y., Yu X-Q., Yin Y-X., Nam K-W., Guo Y-G. Nano Research 8 (2015) 117-128.

[21] Wang L., Song J., Qiao R., Wray L.A., Hossain M.A., Chuang Y-D., Yang W., Lu Y., Evans D., Lee J-J., Vail S., Zhao X., Nishijima M., Kakimoto S., Goodenough J.B. JACS 137 (2015) 2548-2554.

[22] Lee H-W., Wang R. Y., Pasta M., Lee S. W., Liu N., Cui Y. Nat. Commun. 5 (2014) 5280.

[23] Lee H., Kim Y-I., Park J-K., Choi J. W. Chem. Commun. 48 (2012) 8416-8418.

[24] Minowa H., Yui Y., Ono Y., Hayashi M., Hayashi K., Kobayashi R., Takahashi K. I. Solid State Ionics 262 (2014) 216-219.

[25] You Y., Wu X-L., Yin Y-X., Guo Y-G. En. Environm. Sci. 7 (2014) 1643.

[26] Wu X., Deng W., Qian J., Cao Y., Ai X., Yang H. J. Mat. Chem. A 1 (2013) 10130-10134.

[27] Ponrouch A., Marchante E., Courty M., Tarascon J-M., Palacín M.R. Energy Environ. Sci. 5 (2012) 8572-8583.

[28] Ponrouch A., Dedryvère R., Monti D., Demet A. E., Mba J. M. A., Croguennec L., Masquelier C., Johansson P., Palacín M.R. Energy Environ. Sci. 6 (2013) 2361-2369.

[29] Ponrouch A., Monti D., Boschin A., Steen B., Johansson P., Palacín M. R. J. Mater. Chem. A 3 (2015) 22-42.

[30] Tarascon J. M., Guyomard D. Solid State Ionics 64 (1994) 293-305.

[31] Chou S-L., Pan Y., Wang Y-Z., Liu H-K., Dou S-X. Phys. Chem. Chem. Phys. 16 (2014) 20347-20359.

[32] Magasinski A., Zdyrko B., Kovalenko I., Hertzberg B., Byrtovyy R., Huebner C. F., Fuller T. F., Luzinov I., Yushin G. ACS Appl. Mater. Interfaces 2 (2010) 3004-3010.

[33] Chen L., Xie X., Xie J., Wang K., Yang J. J. Appl. Electrochem. 36 (2006) 1099-1104.

[34] Pan H., Lu X., Yu X., Hu Y-S., Li H., Yang X-Q., Chen L. Adv. Energy Mater. 3 (2013) 1186-1194.

[35] Yang L., Ravdel B., Lucht B. Electrochem. Solid-State Lett. 13 (2010) A95-A97.

[36] Piernas-Muñoz M. J., Castillo-Martínez E., Roddatis V., Armand M., Rojo T. J. Power Sources 271 (2014) 489-496.

[37] Gaberscek M., Moskon J., Erjavec B., Dominko R., Jamnik J. Electrochem. Solid-State Lett. 11 (2008) A170-A174.

[38] Iermakova D. I., Dugas R., Palacín M. R., Ponrouch A. J. Electochem. Soc. 162 (2015) A7001-A7007.

[39] Komaba S., Ishikawa T., Yabuuchi N., Murata W., Ito A., Ohsawa Y. ACS Appl. Mater. Interfaces 3 (2011) 4165-4168.

[40] Shkrob I. A., Wishart J. F., Abraham D. P. J. Phys. Chem. C 119 (2015) 14954–14964.

[41] Chen X., Li X., Mei D., Feng J., Hu M. Y., Hu J., Engelhard M., Zheng J., Xu W., Xiao J., Liu J., Zhang J-G. ChemSusChem 7 (2014) 549 – 554.

[42] Markevich E., Salitra G., Fridman, K., R. Sharabi, G. Gershinsky, A. Garsuch, G. Semrau, M. A. Schmidt, D. Aurbach. Langmuir 30 (2014) 7414-7424.

[43] Yeonju P., Su H-S., Hoon H. et al. J. Molecular Structure 1069 (2014) 157-63.

Figures

Figure 1

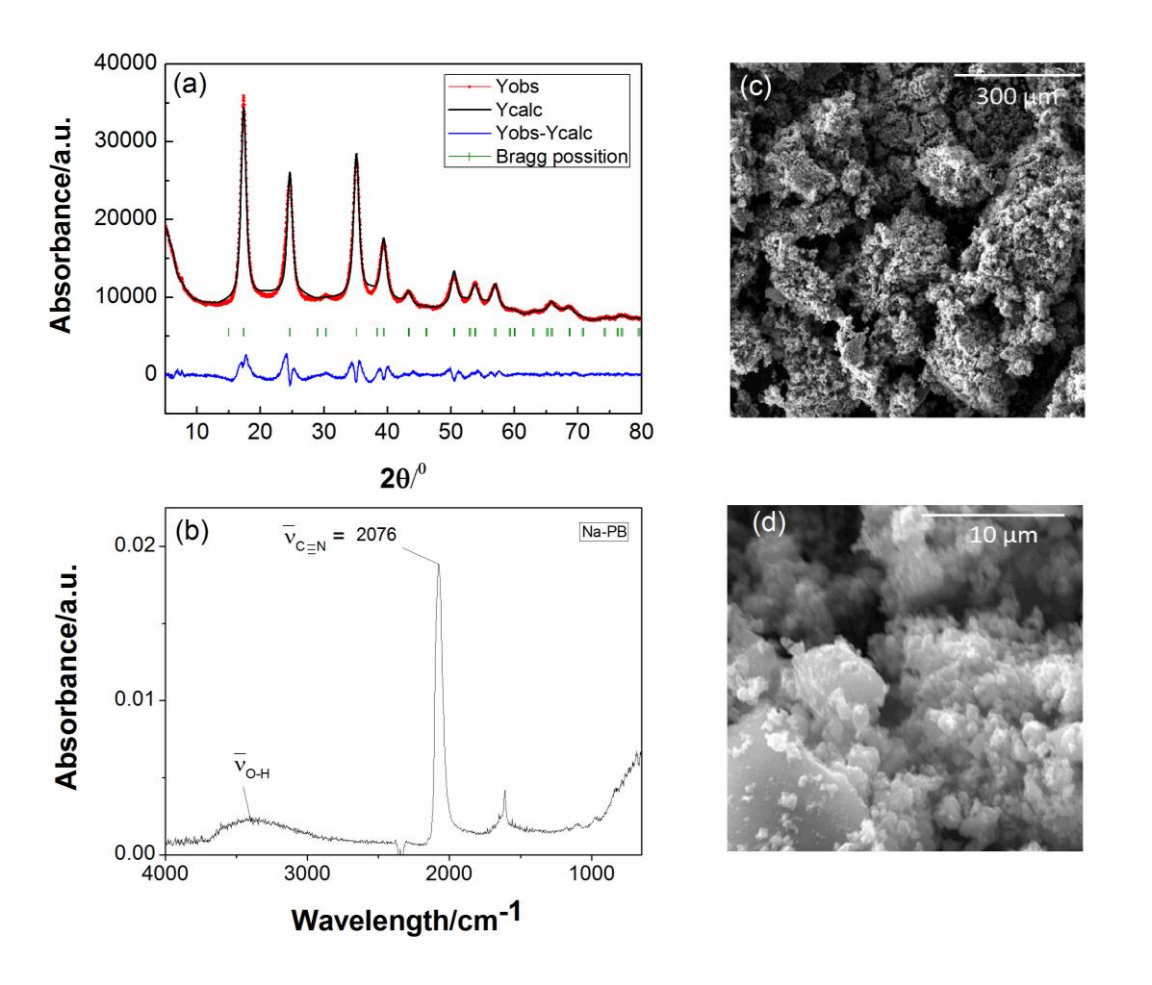

Figure 2

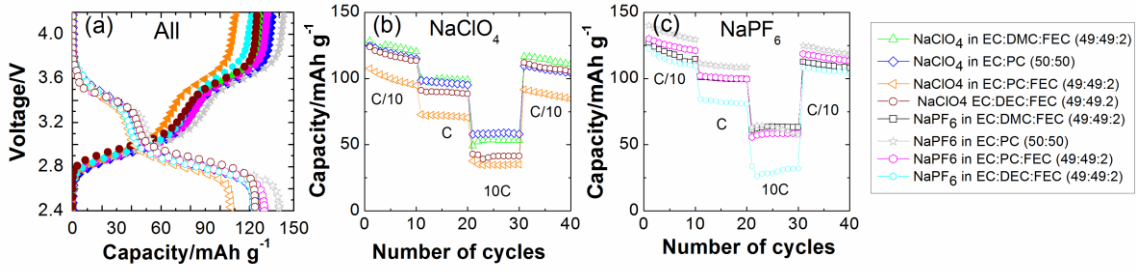

Figure 3

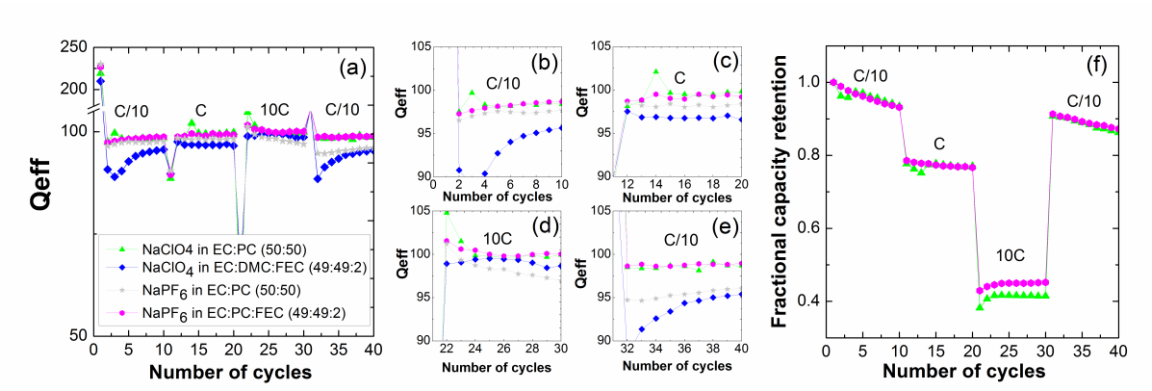

Figure 4

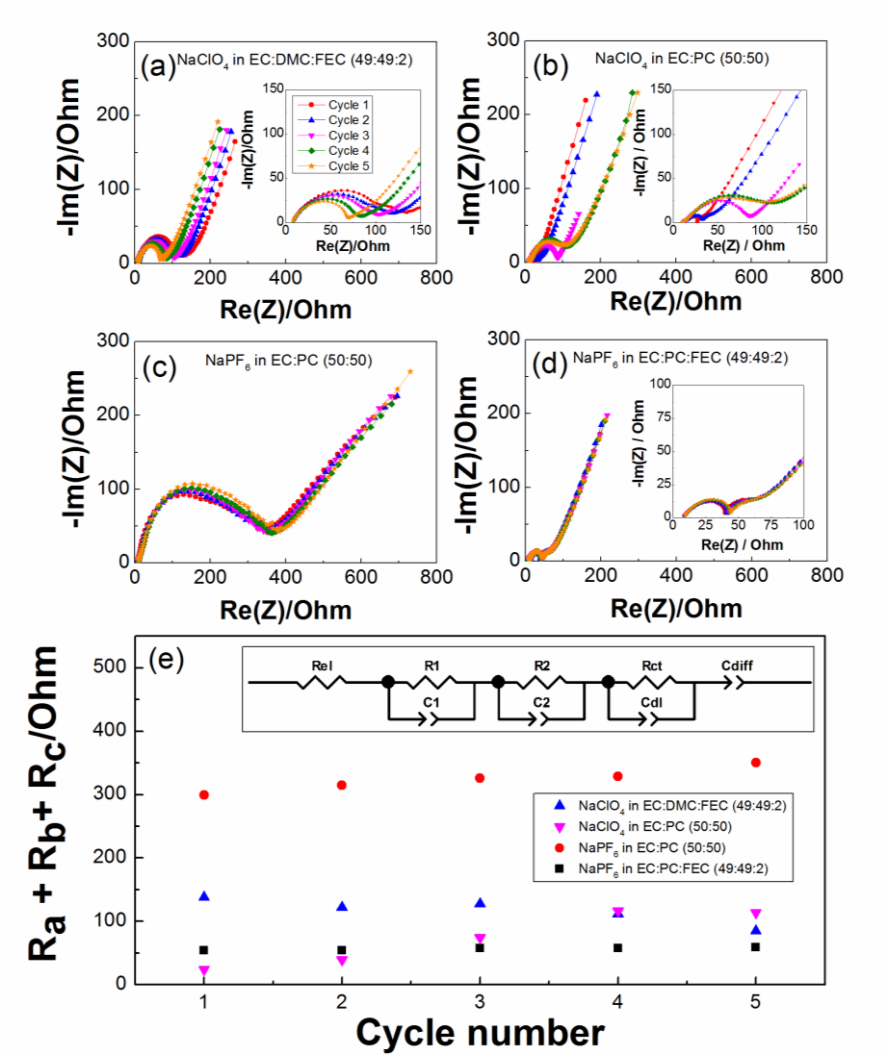

Figure 5

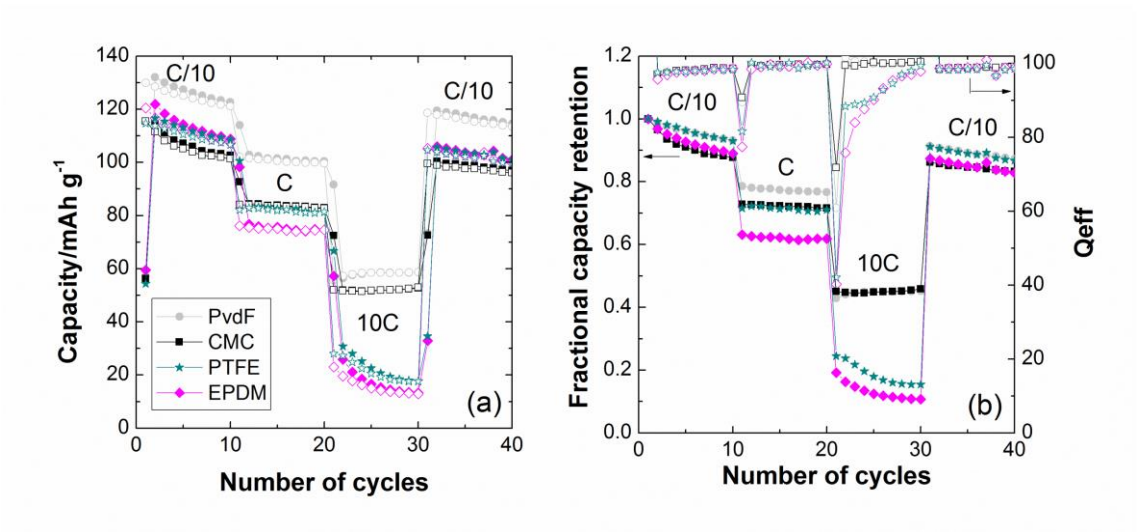

Figure 6

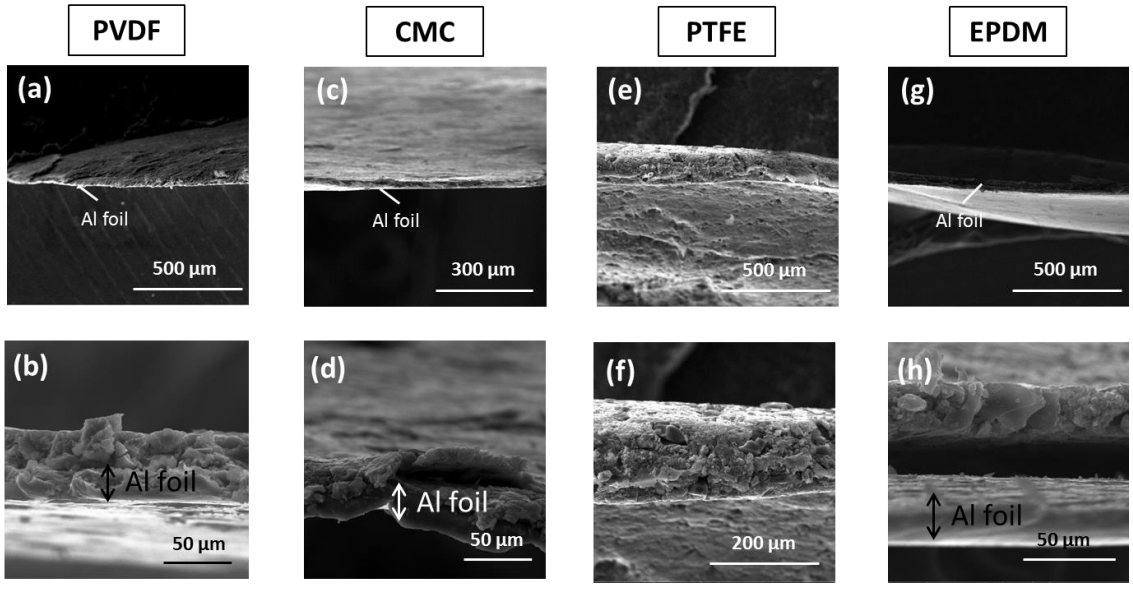

Figure captions

Figure 1. a) Rietveld fit of the XRD pattern of Sodium Prussian Blue (Na-PB) to the XRD pattern of the Prussian Blue (PB) listed in ICSD Karlsruhe Database (nº 162081), space group *Fm*-3*m* (a= 10.2227 (1) Å). Experimental (black) and calculated (red) patterns are shown along with the difference curve (blue). b) IR spectra of Na-PB, $Na_{1-x}Fe^{II}_{1+(x/3)}[Fe^{II}(CN)_6]\cdot yH_2O$, labelling the most characteristic absorption bands. d) SEM images of Na-PB morphology. Note the different scale in the SEM micrographs.

Figure 2. a) First discharge (empty symbols) and second charge (filled symbols) of the Na-PB when cycled using different electrolytes in the voltage window 2.4-4.2 V. b) Electrochemical performance of the Na-PB tested at several C-rate capabilities (being $C_{th,\ Na\text{-}PB}$ = 92.185 mAh/g per $1Na^+$ insertion/f.u.) using the electrolytes containing the $NaClO_4$ salt or the c) $NaPF_6$ salt.

Figure 3. a) Qeff of the NaPB when cycled in the voltage window from 2.4 to 4.2V at various capabilities and using different electrolytes (1M $NaClO_4$ EC: PC 50:50 (blue rhombus), 1M $NaClO_4$ EC: DMC: FEC 49:49:2 (green triangles), 1M $NaPF_6$ EC: PC 50:50 (gray stars) and 1M $NaPF_6$ EC: PC: FEC 49:49:2 (pink hexagons)). For better distinction, a zoom of each range of current densities (C/10, C, 10C and again C/10) has been performed as can be observed in graphs b), c), d) and e), respectively. f) Fractional capacity retention versus number of cycles for the the two best electrolytes, 1M $NaClO_4$ EC: DMC: FEC 49:49:2 (green triangles) and 1M $NaPF_6$ EC: PC: FEC 49:49:2 (pink hexagons), at the C-rates fixed.

Figure 4. Nyquist diagrams of impedance measurements at the EOD for each one of the first 5 cycles of Na-PB *vs*. Na^+/Na at C/10 in a) 1M $NaClO_4$ in EC:DMC:FEC (49:49:2), b) 1M $NaClO_4$ in EC:PC, c) 1M $NaPF_6$ in EC:PC and d) 1M $NaPF_6$ in EC:PC:FEC. Inset in (b), (c) and (d) displays zoom in the high frequency range. Comparison of the

resistances for the 4 different electrolytes tested is presented in e). Inset in (e) shows the equivalent circuit used to fit the data.

Figure 5. a) Specific capacity and b) capacity retention (filled symbols) and Qeff (empty symbols) of Na-PB laminates prepared with different type of binder (PVDF in NMP, CMC in EtOH/H_2O, PTFE in H_2O and EPDM in cyclohexane) at different C-rates, when cycled against Na, using 1M $NaPF_6$ in EC: PC: FEC 49:49:2, in the cut-off voltage from 2.4 to 4.2 V.

Figure 6. SEM images of the cross-section electrodes containing the different binders and their corresponding magnifications: PVDF (a and b), CMC (c and d), PTFE (e and f) and EPDM (g and h).

Tables

1M $NaClO_4$	**1M $NaPF_6$**
EC:PC (1:1)†	**EC:PC (1:1)**†
EC:PC:FEC (49:49:2)	**EC:PC:FEC (49:49:2)**†
ED:DMC (1:1)	ED:DMC (1:1)
EC:DMC:FEC (49:49:2)†	EC:DMC:FEC (49:49:2)
ED:DEC (1:1)	ED:DEC (1:1)
EC:DEC:FEC (49:49:2)	EC:DEC:FEC (49:49:2)
	PC:FEC (98:2)

Table 1. Summary of the electrolytes tested for the electrolyte election.